# Localized optical orbital approach to study localized states of light in photonic crystals

Zhuo Ye,* Xinhua Hu, Ming Li, and Kai-Ming Ho†
*Department of Physics and Astronomy and Ames Laboratory, Iowa State University, Ames, Iowa 50010, USA*

Jiangrong Cao and Mamoru Miyawaki
*Canon Development Americas, Inc., 15975 Alton Parkway, Irvine, California 92618, USA*
(Received 29 September 2008; revised manuscript received 2 April 2009; published 9 July 2009)

A set of localized basis orbitals are presented to locally represent electromagnetic field in photonic crystals. These orbitals are different from the optical Wannier functions. They are the optical parallelism of quasiatomic orbitals in the context of electronic problems. We demonstrate the utility of these localized optical orbitals by recapturing eigenmodes in defected structures. Calculations for cavity modes and dispersion relations of waveguides agree well with the results from plane-wave expansion calculations. This approach also offers interesting physical insight to understand the state of light in ideal photonic crystals as well as defected structures.

DOI: 10.1103/PhysRevB.80.035111 PACS number(s): 42.70.Qs, 42.25.Bs, 71.15.−m

## I. INTRODUCTION

Photonic crystals (PCs), a novel class of optical materials with a periodic dielectric distribution, have attracted much attention in areas of optics and optoelectronics. Due to photonic band-gap effect, light can be localized and manipulated, which facilitates the realization of ultrasmall optical integrated circuits.[1–3] Numerical methods using localized functions such as optical Wannier functions (WFs) (Refs. 4–8) and tight-binding approaches[9–11] have proven to be powerful tools to study the localized states in PCs. Optical Wannier functions, adopted from the electronic theory of solids,[12–15] provide an alternative basis to plane waves to study the localized state of light in PCs. Much interest has been focused on WFs for its highly localized characteristic and usefulness for studying the defected systems. However, considerable steps of iteration are needed to get the maximally localized WFs.[5] In addition, a suitable set of trial functions to start the iteration is essential in this approach. To get these trial WFs, one has to guess the shapes and locations of them. Even with suitable trial WFs, one does not know what the final WFs will look like after iteration, since the iteration process is like a black box and the output WFs may be very different from the input trial functions. As a consequence, these uncertainties make the construction of WFs complex and not so direct.

In this paper we suggest a different basis of highly localized functions as an alternative to WFs. The idea comes from the quasiatomic minimal basis orbitals (QUAMBOs) in the context of electronic theory of solids.[16–18] Like WFs, QUAMBOs are the linear combinations of Bloch orbitals. However, WFs are constructed through minimizing the transverse spread functional,[4,5] yet QUAMBOs are obtained to let themselves be mostly like the free atomic orbitals. The QUAMBOs attained from this scheme contain the adaptation of the basis to the environments such as molecules or crystals, while keeping the essentially quasiatomic character in these environments.[16] The purpose of this paper is to adapt the concept of QUAMBOs to optical systems. Ideal PCs or periodic alternate dielectric materials are like molecules while individual dielectric layers/columns/spheres that build up PCs are like atoms. The optical QUAMBOs should contain information of both "atoms" (individual dielectric blocks) and "molecules" (lattice of these blocks). To construct these QUAMBO-like localized optical orbitals (LOOs), we project Bloch wave solutions to optical states, which are analogous to free atomic orbitals, and orthogonize these projections to make them satisfy the general orthogonalization relation of WFs. Since LOOs and WFs share the same characteristic of localization and orthogonality, theoretically any WF-based scheme can be adapted to LOO method to study defected structures. By comparison between the construction processes of these two bases, we see that LOOs are constructed through direct projection and orthogonalization, while WFs are constructed through iteration. The advantage of projection and orthogonalization lies in that they require much less computer time than iteration. Meanwhile, LOOs and the atomlike orbitals to be projected are very alike, and we can anticipate roughly what the LOOs will look like before they are constructed. But WFs and the trial functions to start iteration may be very different. We do not know what comes out when we put in trial functions. Another superiority of LOOs is its straightforward construction. We do not need to guess anything such as the shape of trial functions.

To illustrate our idea, LOOs are constructed to quantitatively describe the electromagnetic wave localization and propagation in one-dimensional (1D) systems. We chose a 1D system as our first example because this simplest structure offers a most straightforward description of LOO concept. Then this approach is extended to two-dimensional (2D) case, where cavities and straight waveguides are studied. Numerical calculations by other methods[19–22] are also given as a comparison to testify our method. This work also suggests a possibility of using these optical QUAMBOs to study three-dimensional (3D) PCs.

## II. CONSTRUCTION OF LOCALIZED OPTICAL ORBITALS IN 1D SYSTEMS

Consider a 1D PC shown in Fig. 1(a). It is a 1D lattice of dielectric layers in air with dielectric constant $\epsilon=13$. The

 

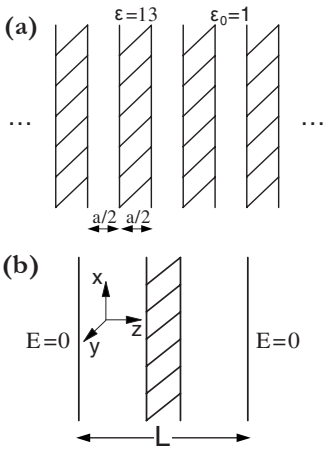


FIG. 1. Structure of (a) a 1D PC of dielectric layers in air and (b) one dielectric layer with a perfect conducting boundary.

thickness of the dielectric layers is one half of the lattice constant $a$. The light that propagates in the $z$ direction can be expressed by the electric field $E(\vec{z})$, which obeys the wave equation

$$\left[\frac{\partial^2}{\partial z^2} + \left(\frac{\omega}{c}\right)^2 \epsilon_p(\vec{z})\right] E(\vec{z}) = 0, \tag{1}$$

where we have assumed a time harmonic dependence, $E(\vec{z},t)=E(\vec{z})\exp(-i\omega t)$, of the electric field with the frequency $\omega$. $\epsilon_p(\vec{z})$ is the dielectric index of the periodic structure $\epsilon_p(\vec{z}+\vec{R})=\epsilon_p(\vec{z})$ and $\vec{R}$ is the lattice vector. Equation (1) has solutions referred to as the Bloch functions, which satisfies the Bloch-Floquet theorem[23]

$$E_{n,\vec{k}}(\vec{z}+\vec{R}) = e^{i\vec{k}\cdot\vec{R}} E_{n,\vec{k}}(\vec{z}), \tag{2}$$

where $n$ and $\vec{k}$ indicate the photonic band index and the wave vector.

To adapt the concept of QUAMBOs to this system, we first need to find solutions which are analogous to free atomic orbitals. However, the scattering nature of light does not allow such localized solutions unless a boundary is enforced to restrain photons from escaping. As Fig. 1(b) shows, we apply a perfect conducting boundary at both sides of a dielectric layer, which is like an "atom." We set the distance $L$ between two ends to be $1.4a$. Note that the value of $L$ cannot be too large compared to $a$, otherwise the atomlike optical orbitals are not well localized. Neither can $L$ be smaller than $a$, to allow interaction between "atoms" (dielectric layers) to give a modulation of light. From our calculation, we find that the optimal value of $L$ ranges from 1.2 to $1.5a$. In this range, the results are not sensitive to this boundary. There are four solutions $E_m^{(0)}(\vec{z})$ $(m=1,2,\ldots,N, N=4)$ in the normalized frequency range $\omega a/(2\pi c)=0.0\sim0.9$, as shown in Fig. 2(a). By projecting $E_m^{(0)}$ to $E_{n,\vec{k}}$, we get the projections[24,25]

$$\tilde{E}_m(\vec{z}) = \sum_{n,\vec{k}} c_{m,n,\vec{k}} E_{n,\vec{k}}(\vec{z}), \tag{3}$$

where coefficients $c_{m,n,\vec{k}}$ are defined as follows:

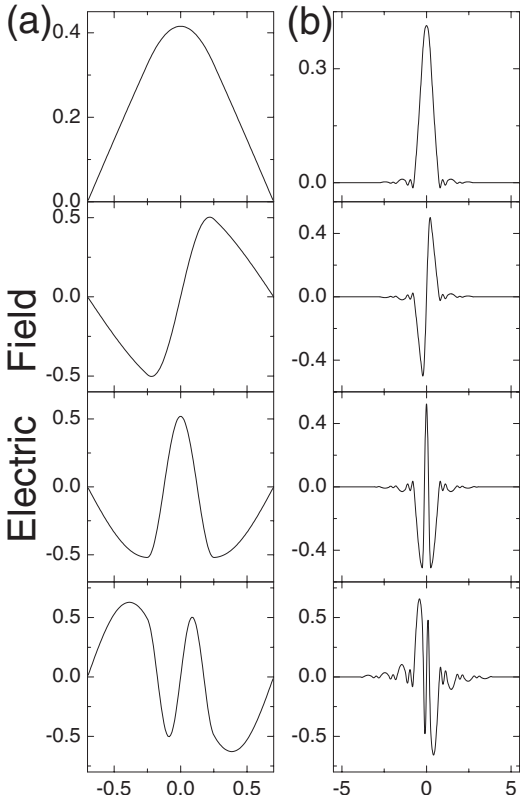


FIG. 2. (a) The first four modes for one dielectric layer with boundary as shown in Fig. 1(b); (b) LOOs constructed from the four modes in (a) and Bloch wave solutions in the first four bands. The horizontal axis is the scale in the unit of lattice constant $a$.

$$c_{m,n,\vec{k}} = \langle E_{n,\vec{k}} | \epsilon_p | E_m^{(0)} \rangle = \int d_{\vec{z}} E_{n,\vec{k}}^*(\vec{z}) \epsilon_p(\vec{z}) E_m^{(0)}(\vec{z}). \tag{4}$$

The integration runs over the entire space. Here we use Bloch waves $E_{n\vec{k}}$ in the first four bands $(n=1,2,\ldots,N, N=4)$. We take 11 $\vec{k}$ points in the first Brillouin zone (BZ). Then we orthonormalize $\tilde{E}_m$ to get a basis $\tilde{E}'_m$,[26,27] which satisfy the relation $\langle \tilde{E}'_m | \epsilon_p | \tilde{E}'_{m'} \rangle = \delta_{mm'}$, and where $\tilde{E}'_m(\vec{z}) = \Sigma_{n,\vec{k}} c'_{m,n,\vec{k}} E_{n,\vec{k}}(\vec{z})$. We pick up the $\vec{k}$ component of $\tilde{E}'_m$ after the above orthogonalization

$$\tilde{E}'_{m,\vec{k}}(\vec{z}) = \sum_n c'_{m,n,\vec{k}} E_{n,\vec{k}}(\vec{z}), \tag{5}$$

and orthonormalize $\tilde{E}'_{m,\vec{k}}$ for each $\vec{k}$ to get a basis $\tilde{E}''_{m,\vec{k}}$, which satisfies $\langle \tilde{E}''_{m,\vec{k}} | \epsilon_p | \tilde{E}''_{m',\vec{k}} \rangle = \delta_{mm'}$, and where $\tilde{E}''_{m,\vec{k}}(\vec{z}) = \Sigma_n c''_{m,n,\vec{k}} E_{n,\vec{k}}(\vec{z})$. Summing up $\tilde{E}''_{m,\vec{k}}$ over $\vec{k}$ we can finally get a set of localized functions $\tilde{E}''_m(\vec{z}) = \Sigma_{\vec{k}} \tilde{E}''_{m,\vec{k}}(\vec{z})$, which can be proven to satisfy the following orthogonality relation

$$\langle \tilde{E}''_m(\vec{z}-\vec{R}) | \epsilon_p(\vec{z}) | \tilde{E}''_{m'}(\vec{z}-\vec{R}') \rangle = \delta_{mm'} \delta_{\vec{R},\vec{R}'}. \tag{6}$$

Following the above steps we construct an orthonormal basis $\tilde{E}''_m(\vec{z})$, i.e., LOOs. Note that here we follow the projection process in the works by Lu *et al.*[16,17] But QUAMBOs in

these works are not an orthogonal set. Beyond projection, we also need an orthogonalization process to make LOOs be an orthonormal basis like WFs. One can easily see that LOOs shares two major characteristics with WFs: the well-localized property and the orthogonality, which is inherited from Bloch functions. Equation (6) has exactly the same form with the orthogonality equation in Refs. 4 and 5. In Fig. 2(b) we plot $\tilde{E}''_m(\vec{z})$ $(m=1,2,\ldots,N,\ N=4)$, which are obtained from the "free atom orbitals" shown in Fig. 2(a). We see that wiggling tails appear in $\tilde{E}''_m(\vec{z})$ as a result of projection and orthogonalization. Instead of jumping to zero from finity at the boundary in original orbitals [see Fig. 2(a)], the magnetic field $H \sim \frac{\partial}{\partial z}E$ naturally undulates steadily to zero in Fig. 2(b). In some cases the wiggling tails extend to long distances and thus break the well-localized property of LOOs. Then we need to introduce virtual orbitals to reduce or get rid of these undesirable wiggling tails.[28]

Since $\tilde{E}''_m(\vec{z})$ owes the orthogonality relation to Eq. (6) just as WFs, we can directly transplant the method, which uses the same orthogonality relation of WFs to calculate the photonic band structure.[4,5] The electric field in Eq. (1) can be expanded in the basis of $\tilde{E}''_m(\vec{z})$

$$E_{\vec{k}}(\vec{z}) = \sum_{m,\vec{R}} C_m e^{i\vec{k}\cdot\vec{R}} \tilde{E}''_m(\vec{z}-\vec{R}), \tag{7}$$

where $C_m$ are undetermined coefficients. By substituting Eq. (7) into Eq. (1) and applying the orthogonality of $\tilde{E}''_m(\vec{z})$ [Eq. (6)], we obtain the following eigenvalue equation:

$$\sum_{m'} \left( \sum_{\vec{R}'} e^{i\vec{k}\cdot\vec{R}'} A^{mm'}_{0\vec{R}'} \right) C_{m'} = \left(\frac{\omega}{c}\right)^2 C_m, \tag{8}$$

where

$$A^{mm'}_{\vec{R}\vec{R}'} = \langle \tilde{E}''_m(\vec{z}-\vec{R}) | -\frac{\partial^2}{\partial z^2} | \tilde{E}_{m'}(\vec{z}-\vec{R}') \rangle$$

$$= \frac{a}{2\pi} \int_{BZ} d\vec{k} e^{i\vec{k}\cdot(\vec{R}-\vec{R}')} \sum_{n=1}^{N} c''^{*}_{m,n,\vec{k}} \left(\frac{\omega_{n,\vec{k}}}{c}\right)^2 c''_{m',n,\vec{k}}. \tag{9}$$

By solving the eigenvalue matrix in Eq. (8), we reproduce the photonic band structure in the LOO basis. The result is shown in Fig. 3. As Eq. (9) indicates, there are two ways to calculate the matrix $A^{mm'}_{\vec{R}\vec{R}'}$. One is to integrate over $\vec{z}$ in real space, the other is to integrate over $\vec{k}$. They both can yield exact reproduction of the photonic band structure. The band structure shown in Fig. 3 is computed from the integral in $k$ space. Solid lines indicate the band structure calculated by plane-wave expansion (PWE) method, and dots by using LOO basis. It can be seen that our method agrees quite well with PWE in the first four bands.

## III. DEFECT STRUCTURES IN 1D PHOTONIC CRYSTALS

In the presence of a defect $\delta\epsilon(\vec{z})$ over the periodic permittivity function $\epsilon_p(\vec{z})$, the electric field Maxwell wave equation Eq. (1) should be rewritten as

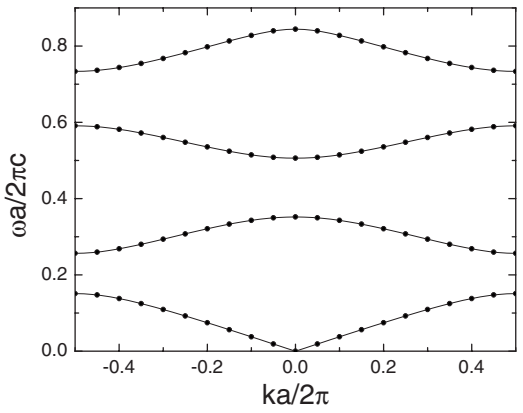


FIG. 3. Band structure of 1D PC in Fig. 1(a) calculated by PWE (solid line) method and reproduced by LOO (dots) method.

$$-\frac{\partial^2}{\partial z^2} E(\vec{z}) = \left(\frac{\omega}{c}\right)^2 \epsilon(\vec{z}) E(\vec{z}), \tag{10}$$

where $\epsilon(\vec{z}) = \epsilon_p(\vec{z}) + \delta\epsilon(\vec{z})$. We expand the electric field in Eq. (10) as follows:

$$E(\vec{z}) = \sum_{m,\vec{R}} C_{m,\vec{R}} \tilde{E}''_m(\vec{z}-\vec{R}), \tag{11}$$

where $C_{m,\vec{R}}$ are coefficients to be determined. By substituting Eq. (11) into Eq. (10) and applying the orthogonality of

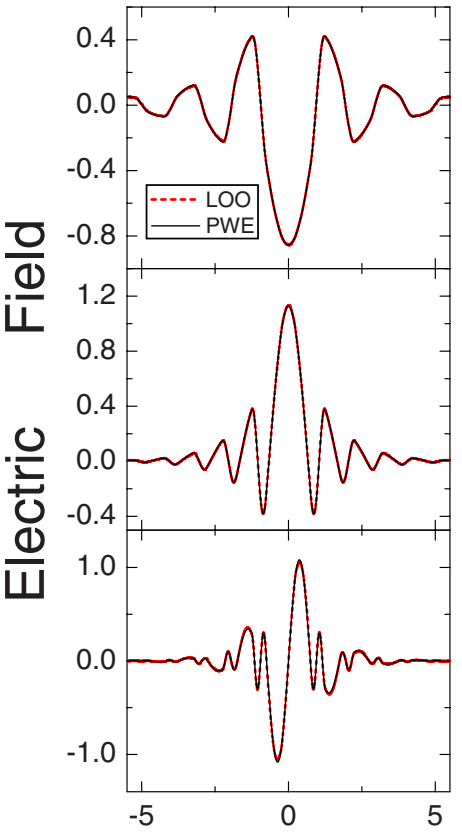


FIG. 4. (Color online) The first three cavity modes from PWE (solid/black) and LOO (dashed/red) calculations. The horizontal axis is the scale in the unit of $a$.

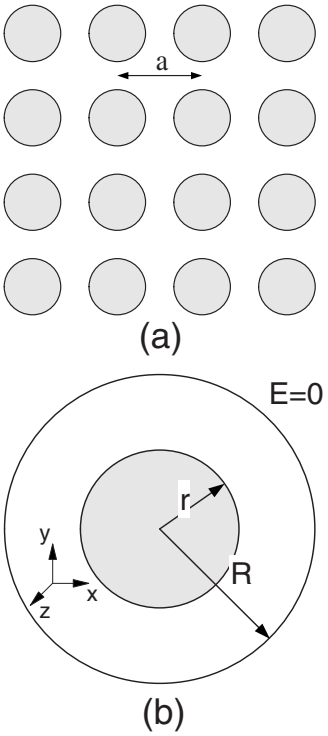


FIG. 5. Structure for (a) a 2D PC with a square lattice of dielectric rods in air, and (b) one dielectric column with a cylindrical perfect conducting boundary.

$\tilde{E}''_m(\vec{z})$, we obtain the following tight-binding matrix equation:

$$\sum_{m',\vec{R}'} A^{mm'}_{\vec{R}\vec{R}'} C_{m',\vec{R}'} = \left(\frac{\omega}{c}\right)^2 \sum_{m',\vec{R}'} \{\delta_{mm'}\delta_{\vec{R}\vec{R}'} + D^{mm'}_{\vec{R}\vec{R}'}\} C_{m',\vec{R}'}, \tag{12}$$

where

$$D^{mm'}_{\vec{R}\vec{R}'} = \langle \tilde{E}''_m(\vec{z}-\vec{R}) | \delta\epsilon | \tilde{E}''_{m'}(\vec{z}-\vec{R}') \rangle = \int d\vec{z} \tilde{E}''^{*}_m(\vec{z}-\vec{R}) \delta\epsilon(\vec{z}) \tilde{E}''_{m'}(\vec{z}-\vec{R}'), \tag{13}$$

and $A^{mm'}_{\vec{R}\vec{R}'}$ is defined as before in Eq. (9). The above is the scheme in Refs. 4 and 5 except that LOOs are used as basis instead of WFs. As a numerical example, we study a structure with one dielectric layer missing. Figure 4 shows the first three eigenmode profiles computed from plane-wave expansion method[19] and our method. In this calculation, we use six LOOs that are constructed from 66 Bloch wave solutions in the first six bands. Exact agreement is achieved in the mode shape and we can hardly see any error. Normalized frequencies for these three cavity modes are 0.24056, 0.37649, 0.67364/0.23991, 0.37615, and 0.67186 given by LOO/PWE calculations, respectively. The maximum relative difference is 0.27%.

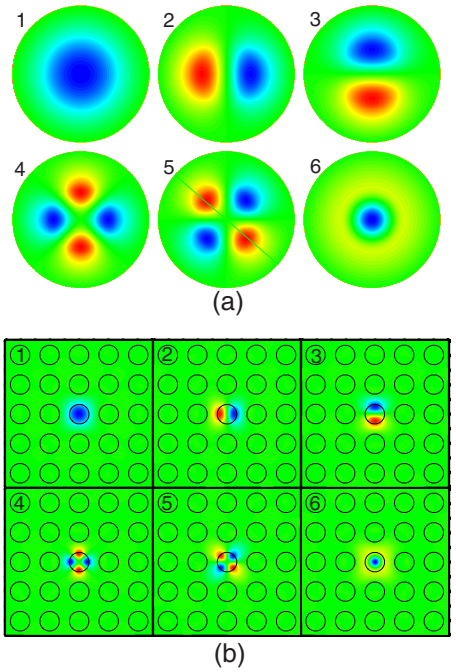


FIG. 6. (Color online) (a) The first six modes for one dielectric column with a cylindrical boundary as shown in Fig. 5(b); (b) LOOs constructed from the six modes in (a) and Bloch wave solutions in the first six bands.

## IV. LOCALIZED OPTICAL ORBITALS IN 2D PHOTONIC CRYSTALS AND DEFECTED STRUCTURES

In parts II and III, we illustrate the concept of LOOs by a 1D example. In this example, each dielectric layer in air can be compared to an isolated atom. These atomlike layers are connected to form a crystal. The state of light that propagates in the crystal can be expanded in the quasiatomlike basis. The basis constructed in this way contains information of both the isolated atoms and lattice made of the atoms. After this 1D example, it is expected to extend our LOO method to 2D cases, where each dielectric pole can be regarded as an atom. In this paper, we restrict ourselves to the case of transverse magnetic (TM)-polarized radiation propagating. However, we would like to point out that this approach can be extended to transverse electric (TE)-polarized radiation as well as light propagation in 3D structures. Consider a square lattice of dielectric columns in air as shown in Fig. 5(a). The cylinder has a dielectric constant 9.0 and a radius $r=0.35a$, where $a$ is the lattice constant. This structure has a 2D photonic band gap from 0.251 to 0.29 and another gap from 0.425 to 0.493 in the normalized frequency $\omega a/2\pi c$.

To find solutions corresponding to free atomic orbitals, again a boundary is needed to restrain light from escaping. We apply a cylindrical perfect conducting boundary to the dielectric cylinder as shown in Fig. 5(b). The radius of the boundary $R$ is set to be $0.7a$. This value is chosen for the same reason as in 1D case. For the structure in Fig. 5(b), there are six TM-polarized solutions $E_z$ ($\vec{z}$ is along the direction of dielectric columns) in the normalized frequency range $\omega a/(2\pi c)=0.0\sim 1.0$, as shown in Fig. 6(a). All of these solutions are products of Bessel functions of first/second kind,

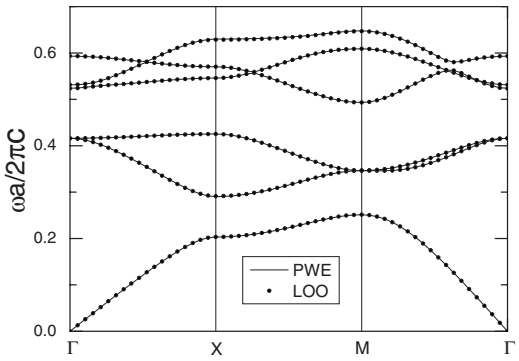


FIG. 7. Band structure (TM polarized) of the 2D PC in Fig. 5(a), calculated by PWE (solid line) method and reproduced by LOO (dots) method.

and an angular function $e^{im\pi}$, where $m$ is an integer. In finding these solutions, we need to consider the symmetry. The second and third solutions are twofolded, while the fourth and fifth fourfolded, and they all appear in pairs. From these six solutions and Bloch eigenstates of PC in the first six bands, we construct six $E_z$ LOOs using the same technique developed in 1D case. We take $7\times7$ $\vec{k}$ points in the whole first BZ, when constructing the LOOs. As indicated in Fig. 6(b), their localization properties as well as the symmetries of the underlying PC structure are clearly visible. We note that through this way of construction, all the LOOs are localized at dielectric rods. This property is different from that of optical WFs, where some of the WFs are localized at air regions.[4,5]

In Fig. 7, we show the photonic band structure in black points reproduced by the E-field LOOs. Solid lines indicate the photonic band structure calculated with 441 plane waves by the PWE method. The solid lines (PWE) and the dots (LOO method) coincide. We use the same method in Refs. 4 and 5 in reproducing the band structure by LOOs.

We consider a cavity with one dielectric cylinder removed from the ideal PC. We apply the E-field LOO method to the calculation of the cavity mode. We take six LOOs in the calculation. As before, the scheme is the same as in Refs. 4 and 5, except that we use LOOs instead of optical WFs. The resonant frequency of the cavity mode in the second band gap is 0.48303 by LOO method versus 0.48017 in normalized frequency $\omega a/2\pi c$ by transfer matrix method (TMM) (see Refs. 21 and 22). The relative difference is 0.60%. In Fig. 8(a), we plot the cavity mode profile computed by LOO method. Mode shape computed by TMM is also plotted as a comparison in Fig. 8(b). A $7\times7$ supercell and 105 plane waves are taken to do the TMM calculation. As we can see in Fig. 8, the mode shapes calculated by the two methods look alike but there is still visible difference. The difference around the edges of supercell can be explained by the interaction between supercells in TMM calculation and thus can be neglected. However, there is noticeable difference in the central and the third peaks that can only be explained by the inaccuracy of LOO method. After testing, we ascribe this error to the inadequate LOOs. If we increase the number of LOOs, the difference is reduced and the whole mode shape is more like what is obtained by TMM.

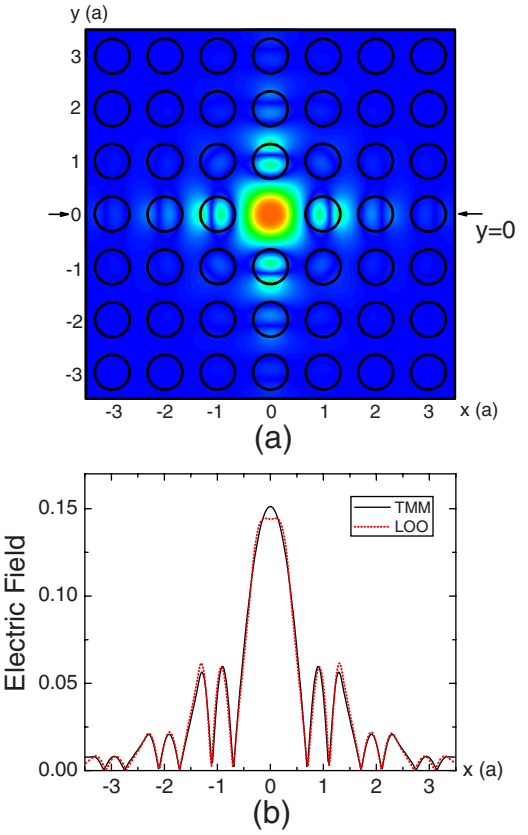


FIG. 8. (Color online) Cavity mode profile. (a) Electric field distribution (magnitude) calculated by LOO method; (b) magnitude of electric field at $y=0$ calculated by TMM (solid/black) and LOO(dots/red) methods.

As our last example, we consider a waveguide consisting of one removed line of dielectric rods. We use the method in Refs. 4 and 5 to calculate the guided mode. Figure 9 shows the dispersion relation of the guided mode in the first gap in the LOO method (dots) and in PWE (solid lines). As indicated in the figure, the solid lines and the dots coincide very well. We take six LOOs in LOO calculation, and a $7\times1$ supercell and 105 plane waves in PWE calculation.

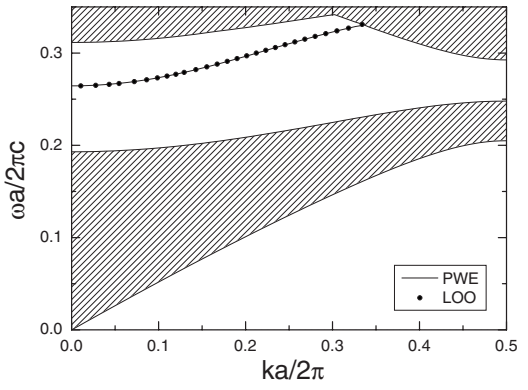


FIG. 9. Dispersion relation of guided mode calculated by PWE (solid line) and LOO (dots) methods.

## V. CONCLUSIONS

In conclusion, we develop a QUAMBO-like, E-field LOO method to study localized states of defected PCs. We have demonstrated the applicability, precision, and efficiency of LOO method to 1D and 2D (TM polarization) PCs with planar, point, and line defects. The structures that we took as examples both have analytical solutions corresponding to free atomic orbitals. However, for those structures that do not have analytical free-atomlike solutions such as lattice of arbitrary shaped poles, we need to use numerical methods such as finite difference time domain[29] to find these solutions. This will add little to calculation burden, since it is over a region that is comparable to one unit cell. Our method can be extended to the description of TE-polarized radiation in 2D PCs as well as to the propagation of optical waves in 3D PCs, by applying the same scheme of optical WFs in Ref. 5. The reason which allows us to do so is that the only difference between LOO and optical WF method lies in the way of construction of LOOs/WFs. Since the two bases share the same characteristic of localization and orthogonality, theoretically any WF-based scheme (e.g., see Refs. 4, 5, and 7) can be adapted to LOO method. Our future work includes study of TE-polarized propagation in 2D PCs and propagation of electromagnetic waves in 3D PCs by applying LOO method.

## ACKNOWLEDGMENTS

Z.Y. thanks W. C. Lu, Y. Yao, and C. Z. Wang for discussions on QUAMBOs in Refs. 16 and 17. This work was supported by the Department of Energy under Project No. DE-AC-02-05CH11231. The Ames Laboratory is operated for the U.S. Department of Energy by Iowa State University under Contract No. W-7405-ENG-82.

*zye@iastate.edu
†kmh@ameslab.gov

[1] E. Yablonovitch, Phys. Rev. Lett. **58**, 2059 (1987).
[2] J. D. Joannopoulos, P. R. Villeneuve, and S. Fan, Nature (London) **386**, 143 (1997).
[3] A. Mekis, J. C. Chen, I. Kurland, S. Fan, P. R. Villeneuve, and J. D. Joannopoulos, Phys. Rev. Lett. **77**, 3787 (1996).
[4] K. Busch, S. F. Mingaleev, A. Garcia-Martin, M. Schillinger, and D. Hermann, J. Phys.: Condens. Matter **15**, R1233 (2003).
[5] H. Takeda, A. Chutinan, and S. John, Phys. Rev. B **74**, 195116 (2006); Europhys. Lett. **76**, 222 (2006).
[6] J. P. Albert, C. Jouanin, D. Cassagne, and D. Bertho, Phys. Rev. B **61**, 4381 (2000).
[7] Y. Jiao, S. Fan, and D. A. B. Miller, IEEE J. Quantum Electron. **42**, 266 (2006); Opt. Lett. **30**, 141 (2005).
[8] D. M. Whittaker and M. P. Croucher, Phys. Rev. B **67**, 085204 (2003).
[9] A. Yariv, Y. Xu, R. K. Lee, and A. Scherer, Opt. Lett. **24**, 711 (1999).
[10] M. Bayindir, B. Temelkuran, and E. Ozbay, Phys. Rev. Lett. **84**, 2140 (2000).
[11] D. P. Fussell and M. M. Dignam, Appl. Phys. Lett. **90**, 183121 (2007).
[12] G. H. Wannier, Phys. Rev. **52**, 191 (1937).
[13] W. Kohn, Phys. Rev. B **7**, 4388 (1973).
[14] N. Marzari and D. Vanderbilt, Phys. Rev. B **56**, 12847 (1997).
[15] I. Souza, N. Marzari, and D. Vanderbilt, Phys. Rev. B **65**, 035109 (2001).
[16] W. C. Lu, C. Z. Wang, T. L. Chan, K. Ruedenberg, and K. M. Ho, Phys. Rev. B **70**, 041101(R) (2004).
[17] W. C. Lu, C. Z. Wang, M. W. Schmidt, L. Bytautas, K. M. Ho, and K. Ruedenberg, J. Chem. Phys. **120**, 2629 (2004).
[18] T. L. Chan, Y. X. Yao, C. Z. Wang, W. C. Lu, J. Li, X. F. Qian, S. Yip, and K. M. Ho, Phys. Rev. B **76**, 205119 (2007).
[19] K. M. Ho, C. T. Chan, and C. M. Soukoulis, Phys. Rev. Lett. **65**, 3152 (1990).
[20] P. Lalanne, Phys. Rev. B **58**, 9801 (1998).
[21] Z. Y. Li and L. L. Lin, Phys. Rev. E **67**, 046607 (2003); Z. Y. Li and K. M. Ho, Phys. Rev. B **68**, 155101 (2003).
[22] M. Li, Z. Y. Li, K. M. Ho, J. R. Cao, and M. Miyawaki, Opt. Lett. **31**, 262 (2006); Z. Ye, X. Hu, M. Li, K. M. Ho, and P. Yang, Appl. Phys. Lett. **89**, 241108 (2006).
[23] J. D. Joannopoulos, S. G. Johnson, J. N. Winn, and R. D. Meade, *Photonic Crystals: Molding the Flow of Light* (Princeton University, Princeton, NJ, 1995).
[24] For this 1D structure, since the bands are separate from each other, actually the projection can be simplified as projecting $E_n^{(0)}$ to $E_{n,\vec{k}}$. That is, calculating a LOO only requires the states in one band. However, for the more general case of 2D and 3D structures, the bands are always entangled. So we need to project $E_m^{(0)}$ to $E_{n,\vec{k}}$ for all $(m,n)$s. Here we write down the general form of projection [Eq. (3)] to accommodate 2D and 3D structures.
[25] In this projection, all bands are included. Yet our method is exact not only in the limit that all bands are included in the projection but also in cases that only some of bands are included, as far as a perfect crystal is considered.
[26] We define a general linear transformation $T$ for the basis $\Phi$ to go to a new basis $\Phi'$: $\Phi'=\Phi T$. The basis $\Phi'$ will be orthonormal if $\langle\Phi'|\Phi'\rangle=\langle\Phi T|\Phi T\rangle=T^\dagger\langle\Phi|\Phi\rangle T=I$. Define a Hermitian matrix $M=\langle\Phi|\Phi\rangle$. The matrix $T=M^{-1/2}=VD^{-1/2}V^\dagger$, where $D$ is the diagonal matrix of eigenvalues of $M$ and $V$ is the full matrix whose columns are the corresponding eigenvectors, gives an orthonomal transformation. For more details on this symmetric orthogonalization, see Ref. 27.
[27] P.-O. Löwdin, Ark. Mat., Astron. Fys. **35**, 9 (1947); V. Srivastava, J. Phys. A **33**, 6219 (2000).
[28] To get virtual orbitals, we use the same method as in Ref. 16. In this paper all orbitals are real/occupied, which is a specific case of the method in Ref. 16 [there are no virtual Bloch orbitals $\varphi_p$ in Eq. (1) in Ref. 16].
[29] *Computational Electrodynamics: The Finite-Difference Time-Domain Method*, edited by A. Taflove (Artech House, Boston, MA, 1995).